Mitigation of ground borne noise in rock railway tunnels - Part II: Full scale tests

R. Cleave, C. Madshus & L. Grande
Department of Geomechanics, Norwegian Geotechnical Institute, Oslo, Norway

Arild Brekke & Karin Rothschild
Brekke & Strand akustikk as, Oslo, Norway

ABSTRACT: Railway traffic in shallow depth rock tunnels can give unacceptable levels of ground borne noise in buildings above the tunnel. For such a tunnel under construction in Norway a project was commissioned by the Norwegian Rail Administration (JBV) to design the most cost effective track that satisfied the prescribed residential sound levels. A component of this project was a series of full scale tests. This, the second part of a two part paper, discusses these full scale tests and compares the measured results against those predicted by the simulation work of the first part of the paper. For each of the seven track substructures tested the acceleration of the rail, sleeper, tunnel floor and tunnel wall were recorded, in addition to the acceleration at various depths throughout the track substructure. Vibration and sound were also measured in the houses above the tunnel. The input to the entire system was via a fully laden freight wagon which had a dynamic excitation force applied to one axle. This force was excited by a hydraulic actuator which, operating under force control, delivered excitation in sweeps of one-third octave bands that covered the relevant frequency range. This paper presents the testing program and corresponding results, and compares these results with the predictions of the companion paper.

1 INTRODUCTION

The origin of structure borne sound from railway traffic is the dynamic variation in the vertical contact forces between rail and wheel. These varying dynamic forces are caused by irregularities in the rail and wheel surfaces, out of round wheels, wheel eccentricity and vibration of the rolling stock itself. The forces are transmitted through rail and sleeper, down through the track structure and into the rock in the tunnel floor. The vibrations generated by these forces are then transmitted through the rock to the foundations of the buildings on the surface, where, if the levels are high enough, vibrating floors and wall surfaces radiate audible sound.

The section of tunnel in question has a rock overburden of approximately 5m. Along this section an extra 1.6m of rock was excavated from the tunnel floor, providing more depth for vibration transmission countermeasures. The tests were performed in a nearly complete part of this section.

Based upon the design model developed in Cleave et al. 2005 three track designs using the

Table 1: The seven full scale test tracks.

	Track A	**Track B**	**Track C**	**Track D**	**Track E**	**Track F**	**Track G**
Axle load	22.5kN	22.5kN	22.5kN	22.5kN	22.5kN	22.5kN	22.5kN
Wheel	1200kg, EVA railpad	1200kg, EVA railpad	1200kg, EVA railpad	1200kg, Pandrol railpad	1200kg, Pandrol railpad	1200kg, Elastic rail fastener	1200kg, Pandrol railpad
Sleeper	300kg	300kg	300kg	300kg	300kg	300kg	300kg
Ballast	0.6m	0.6m	0.6m, in two layers	0.6m	0.6m	0.6m	0.6m
Ballast mat	0.04m, 20MN/m^3	0.085m, 24MN/m^3		0.085m, 24MN/m^3			
Extra rockfill				1.6m poor quality, well-graded rockfill	1.6m poor quality, well-graded rockfill	1.6m poor quality, well-graded rockfill	0.8m LECA, 0.8m poor quality, well-graded rockfill
Ballast mat					0.085m, 24MN/m^3	0.085m, 24MN/m^3	0.085m, 24MN/m^3
Levelling	100mm	100mm	100mm	100mm	100mm	100mm	100mm

extra 1.6m of excavated depth were selected for full scale testing. In addition to these there were three control tracks of normal depth (without the extra 1.6m excavation), and a clone of one of the deeper designs but with an elastic rail fastening system. Table 1 lists each of these seven test tracks. Each track section was approximately 8 metres long, with all seven laid end on end. A single axle freight wagon was used for the loading and excitation of the track, with concrete weights added to achieve full static axle load and a servo-hydraulic actuator to deliver the dynamic load. The dynamic load was applied to simulate the actual dynamic loads that occur on a moving train.

2 FULL SCALE TESTS

The seven tracks were tested consecutively over two days. For each track the dynamic load sequences were repeated in order to check the repeatability of the system and to reduce the effect of other external influences influences (for example rail traffic in the neighbouring tunnel).

The data from sensors in the tunnel were logged on one system and those in the houses were logged on another, with a common channel used for synchronisation. The freight wagon was lifted onto and loaded at each track, and the accelerometers, load cells and static measurement system were moved and reinstalled at each track as the wagon was moved.

2.1 Actuation

The dynamic load was applied to one of the wheel axles by means of a servo hydraulic actuator which acted against a heavy, softly sprung mass. In all of the test series except one the actuator was installed near the wheel set on one side of the wagon, while in one test series the actuator

was mounted in the middle of the axle. Figure 1 depicts a schematic drawing of the system and a photo of the setup. The dynamic capacity of the actuator was ±10kN, and this was fully

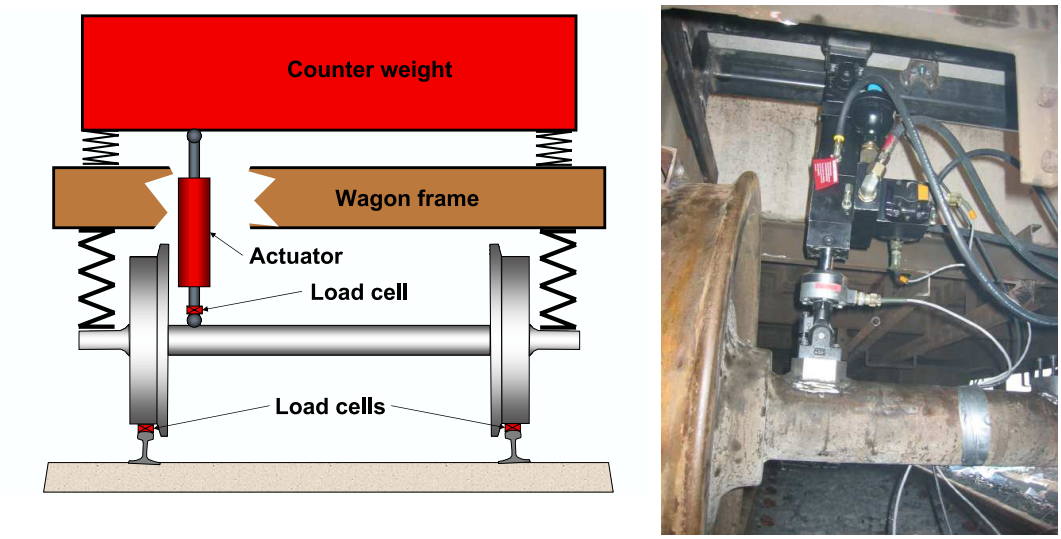

(a) Dynamic loading mechanism.

(b) Photo of actuator.

Figure 1: System for generating and measuring dynamic force.

utilised over the entire frequency spectrum.

For each track three dynamic load sequences were applied; the first of these was a series of pure tones at each of the 1/3 octave bands with centre frequencies from 20Hz to 315Hz, while the other two were a series of band limited random noise such that each part of the series encompassed the 1/3 octave bands with centre frequencies from 31.5Hz to 315Hz. The total duration of the pure tone sequence was 16 minutes, while the random sequences were 10 minutes long.

2.2 Sensing

Accelerometers were placed on the rail and the sleeper, at various depths throughout the track substructure, on the tunnel floor, on the tunnel wall and on the foundation of the buildings above the tunnel. Load cells under each wheel of the dynamically loaded axle measured the dynamic component of the wheel-rail force, while a load cell mounted in the actuator measured the dynamic input load and gave feedback to the actuator control loop. The static deflection of each track was measured under loading of the wagon using a stationary laser beam pointing at a CCD array attached to the rail. Microphones were placed in the tunnel and in the houses. Data from all of these channels, as well as load and stroke data from the hydraulic actuator, were logged simultaneously. Figure 2 sketches a typical track with instrumentation.

The accelerometers in the track substructure were attached with magnets to steel pedestals that were fastened to aluminium plates. These plates were either embedded in the track substructure material or, in the case of the ballast mats, placed on top of the mat. The combined weight of the plate, pedestal and sensor was loosely matched to the density of the rockfills, to reduce the impedance contrast between the surrounding substructure and the sensor assembly. Plastic riser pipes that were vibrationally isolated from the substructure allowed for installation and removal of the accelerometers at the various test tracks. The accelerometers on the tunnel floor were mounted in the same way but with the aluminium plates set in concrete to the tunnel

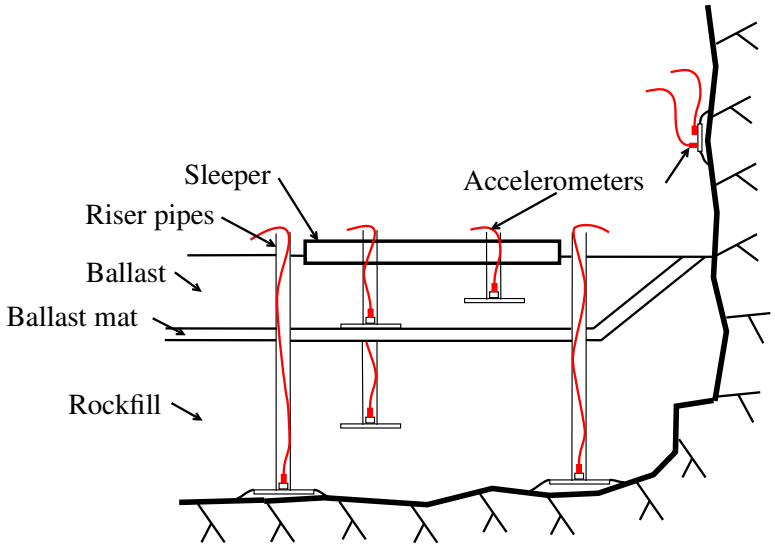

Figure 2: Typical track section with instrumentation.

floor. The tunnel wall accelerometers and the laser were fastened to preinstalled rock bolts.

3 RESULTS

In the results that follow the Insertion Loss is used as the main measure with which to compare the track designs. This insertion loss is the ratio of the transfer function of a reference track over that of another track:

$$IL(\omega) = \left| \frac{H_{\text{ref}}(j\omega)}{H(j\omega)} \right|, \tag{1}$$

where $H_{\text{ref}}(j\omega)$ is the transfer function for the reference track and $H(j\omega)$ the transfer function for the track under evaluation. The input to the transfer functions in this work is the rail force, where this is computed by

$$Q_{\text{in}} = \sqrt{Q_{\text{left}}^2 + Q_{\text{right}}^2}, \tag{2}$$

where Q_{left} is the force on the left rail and Q_{right} the force on the right. The output of the transfer functions is the acceleration of either the tunnel floor or the tunnel wall. In the case of the tunnel floor acceleration the accelerometer on the same side as the actuator has been used. To simplify the following results somewhat only the results from one of the randomised sine sweeps has been used. The two randomised results produced better results that the pure tone sweeps and were very repeatable.

3.1 Accelerations throughout track structure

Figure 3 plots the measured and simulated accelerations for the sleeper, the tunnel floor and several layers of the substructure of Track D. The simulated accelerations have been produced using the one dimensional model developed in Cleave et al. 2005. This model comprises the suspended railcar, rolling mass, rail, sleeper, railway substructure (ballast, ballast mats and backfill) and tunnel floor. The simulation results shown in Figure 3 (dashed lines) were calculated by applying the actuator force, as measured in each individual test, to the rolling mass component of the model. While the simulation performs very well in an overall sense there is

deviation at certain frequencies. Of particular note is the high frequency deviation in the rock acceleration, as this is present in all of the tracks except Tack C.

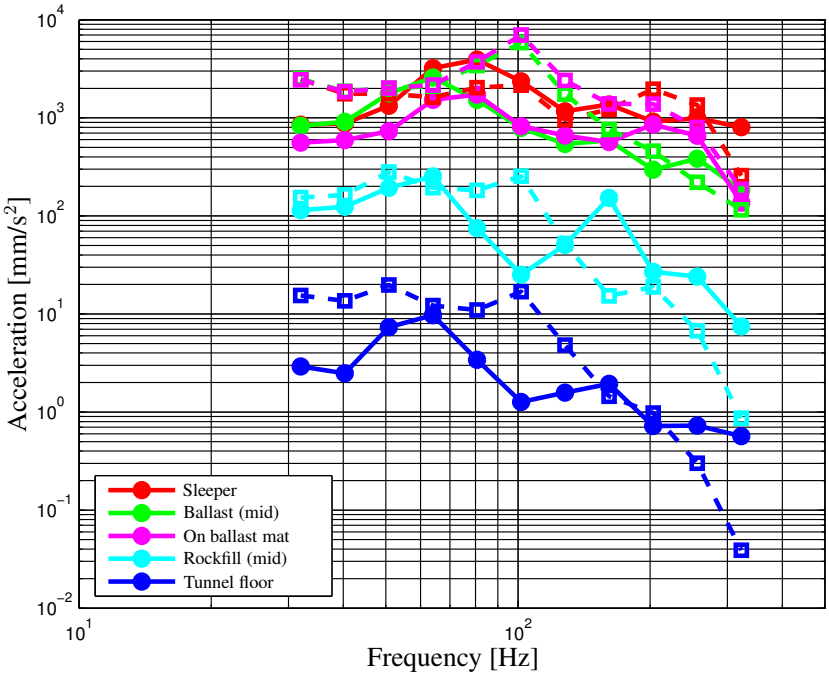

Figure 3: Measured and simulated accelerations for the sleeper, tunnel floor and substructure, Track D. The dashed lines are the simulated results.

3.2 Insertion loss

Figure 4 plots the measured and simulated insertion losses for each track, using the transfer function from the rail force to the tunnel floor as the basis for the insertion loss. Track C is used as the reference track, so that the insertion loss curves show how much better (in terms of noise reduction) each track is in comparsion to Track C. With the exception of Track E the simulated insertion loss agrees well with the measured results. The consistent deviation at high frequencies is a result of the error in simulated high frequency accelerations of the tunnel floor (see Figure 3).

Figure 5 compares the measured results for all tracks. While neither track was better than the rest over the entire frequency range, it is clear that Track D performed most favourably. Track G performed very well up to 100Hz but very poorly at higher frequencies. Tracks A and B differed only in the type of ballast mat used, so it is interesting to note that the softer mat ($k = 20$MN/m^3) produced 4-9dB more isolation (up to 100Hz) than the stiffer mat. Brekke and Gåsemyr 2005 discusses ballast mats and their stiffness requirements, with special regard to Norwegian conditions.

3.2.1 Tunnel wall

Figure 6 plots the measured insertion loss, using the tunnel wall acceleration as the transfer function output (seeEqn. (1)), for each track. At frequencies above 160Hz the vibration transmission increases with frequency for all test sites apart from site C, where it decreases some-

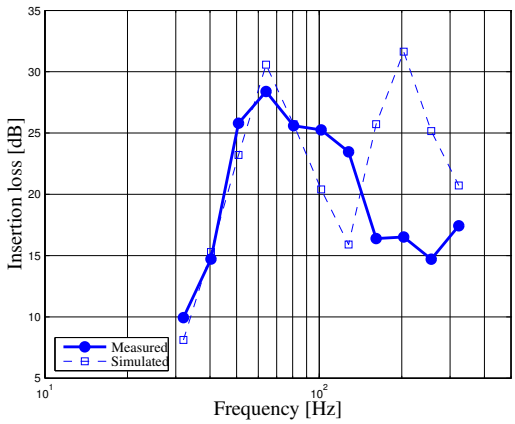

(a) Track A.

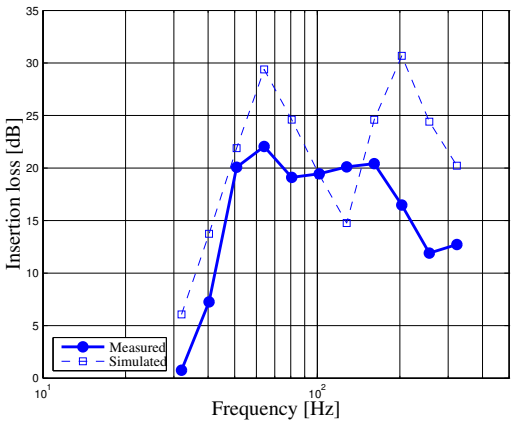

(b) Track B.

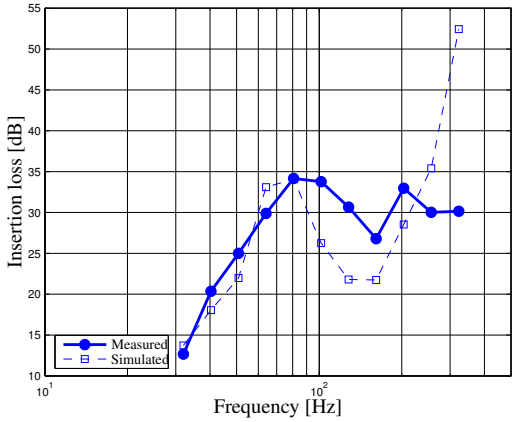

(c) Track D.

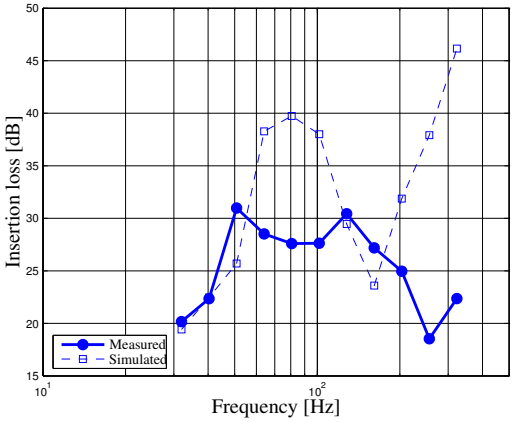

(d) Track E.

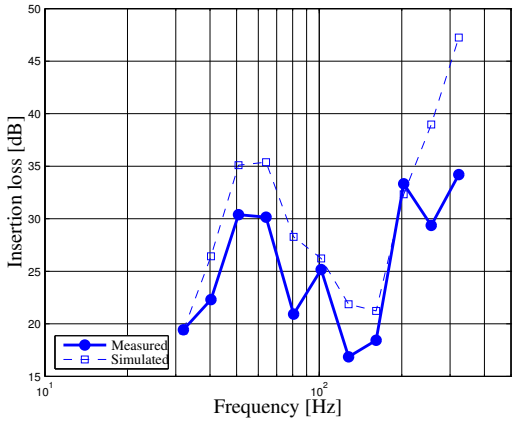

(e) Track F.

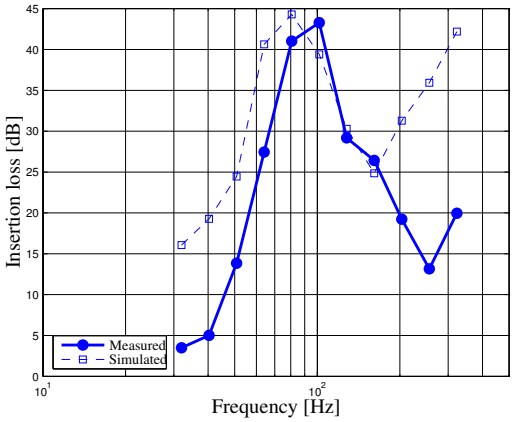

(f) Track G.

Figure 4: Measured and simulated insertion losses, using the tunnel floor as output and the rail force as input in the insertion loss calcuation. The reference track is Track C.

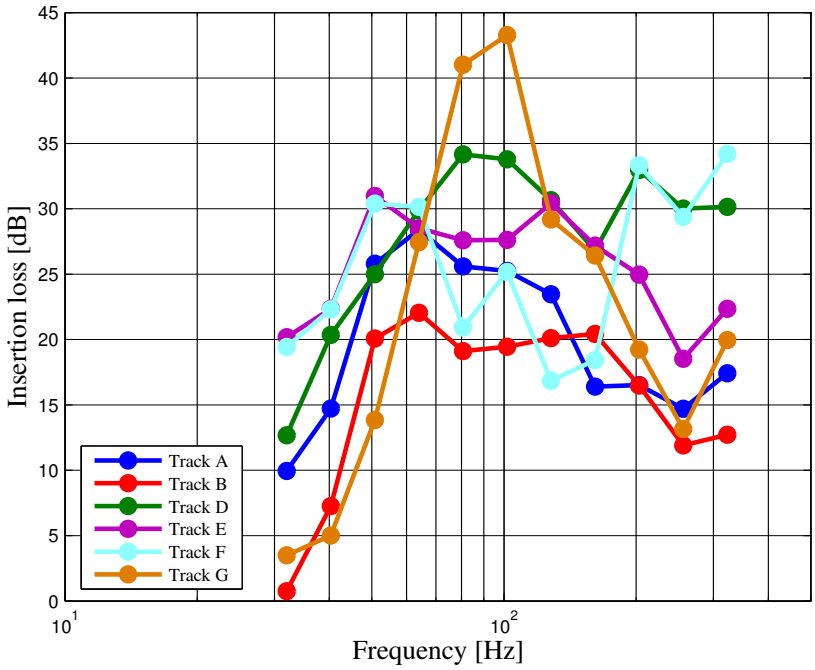

Figure 5: Measured insertion loss for all tracks, using the rail force to tunnel floor transfer function. The reference track is Track C.

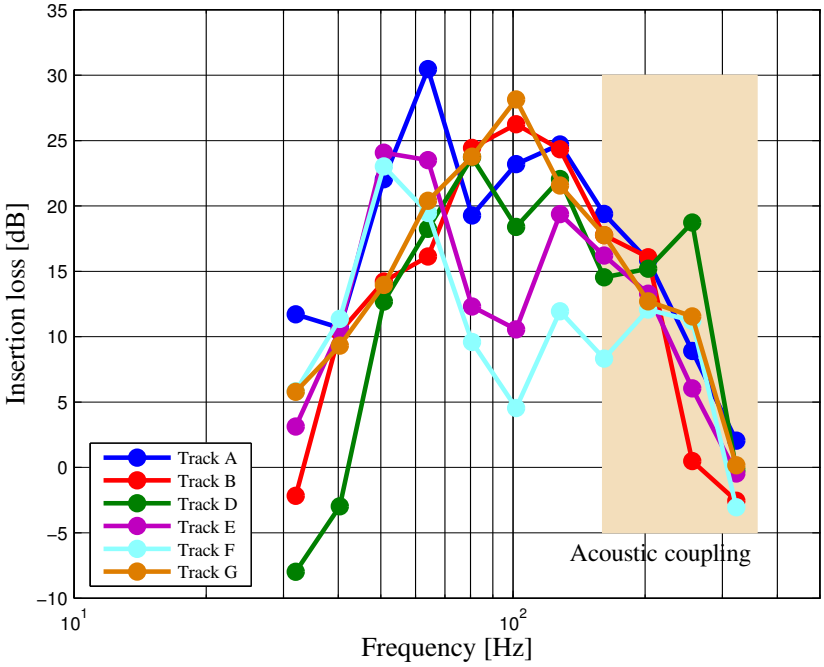

Figure 6: Measured insertion loss for all tracks, using the rail force to tunnel wall transfer function. The reference track is Track C.

what. This causes the sharp decrease in insertion loss shown in Figure 6. This decrease, which implies that the insertion loss for all tracks decreases to nearly zero at 300Hz (i.e. no structure borne sound reducing effect), is not in accordance with what is measured on the tunnel floor. A sound test carried out subsequently showed that the vibrations on the tunnel wall from 160Hz and upwards for sites A, B, D, E, F and G were in fact influenced more by the sound pressure in the tunnel than by the dynamic force on the rail. For Site C, on the contrary, the mechanical transmission path was so good that the vibrations on the tunnel wall were mainly comprised of vibrations induced by the rail force, not only for the lower frequencies as for the other sites, but over the entire frequency range. The curves for the insertion loss in Figure 6 are therefore not valid above 160Hz.

4 CONCLUSIONS

The model developed in Cleave et al. 2005 has been shown to be effective in the simulation and comparison of different railway substructures. The insertion losses predicted by the model and measured in the full scale tests match well for most of the frequency range under consideration, but deviate at higher frequencies. This was largely due to over estimation of the tunnel floor acceleration for the reference track and under estimation of the tunnel floor acceleration in the other tracks.

While no one track design was better than the others over the entire frequency range, the design of Track D ranked highly over the entire range, and was therefore chosen as the best solution. The wall accelerations measured were influenced at high frequency by the noise created by the tests. This caused incorrect estimation of the insertion loss, at least at high frequencies.

The data logged in this work can be used in more detailed analysis of the system, especially with regard to further development of the simulation model used here aas well as in the development of more sophisticated models.

5 ACKNOWLEDGEMENTS

The authors would like to thank the Norwegian Rail Administration (JBV) for the funding of this work, and Norconsult AS and Mica AS as for their teamwork and contributions.

REFERENCES

Brekke, A. and Gåsemyr, H., 2005. *Revised requirements for stiffness of ballast mats in new Norwegian railway lines*. In 7th International Conference on the Bearing Capacity of Roads, Railways and Airfields.

Cleave, R., Madshus, C., Grande, L., Brekke, A. and Rothschild, K., 2005. *Mitigation of ground borne noise in rock railway tunnels - Part I: Track design and simulation*. In 7th International Conference on the Bearing Capacity of Roads, Railways and Airfields.